ISSN 0023-1584, Kinetics and Catalysis, 2009, Vol. 50, No. 4, pp. 587–596. © Pleiades Publishing, Ltd., 2009.
Original Russian Text © V.A. Zazhigalov, E.A. Diyuk, V.V. Sidorchuk, T.I. Mironyuk, 2009, published in Kinetika i Kataliz, 2009, Vol. 50, No. 4, pp. 608–617.

Synthesis of Vanadium–Phosphorus Oxide Catalysts Supported on Pyrogenic Silica and Titanium Dioxide

V. A. Zazhigalov, E. A. Diyuk, V. V. Sidorchuk, and T. I. Mironyuk

Institute of Sorption and the Problems of Endoecology, National Academy of Sciences of Ukraine, Kiev, Ukraine
e-mail: zazhigal@ispe.kiev.ua

Received March 6, 2008

Abstract—Various methods for the preparation of vanadium–phosphorus oxide (VPO) catalysts supported on aerosils A-300 and A-50 and TiO_2 were studied: a traditional method (in an organic solvent under varying the support addition time, the nature of the reducing agent, and the degree of reduction of vanadium oxide) and barothermal and mechanochemical syntheses. With the use of XRD analysis, it was found that the composition of the resulting VPO phase depends on the time of support addition to the synthesis and the temperature of thermal treatment. Conditions for the formation of a supported phase of $VOHPO_4 \cdot 0.5H_2O$, the precursor of the active component $(VO)_2P_2O_7$, were determined. The presence of vanadium in an oxidation state of +4 was demonstrated using EPR and UV–VIS spectroscopy. The specific surface areas and pore structures of the synthesized catalysts were determined. The catalytic properties of samples in the reactions of *n*-butane oxidation in an excess of the hydrocarbon and oxidative ethane dehydrogenation were studied. It was found that, as compared with traditional bulk VPO catalysts, the use of the synthesized supported VPO catalysts made it possible to improve the process characteristics of *n*-butane oxidation and did not change these characteristics in the reaction of oxidative ethane dehydrogenation.

DOI: 10.1134/S002315840904017X

INTRODUCTION

Vanadium–phosphorus oxide (VPO) systems are well known as efficient catalysts for the selective oxidation of light hydrocarbons, for example, *n*-butane oxidation to maleic anhydride [1–9], and this process has been commercialized based on these catalysts. The vanadyl pyrophosphate phase $(VO)_2P_2O_7$, which results from the activation of its precursor, vanadyl hydrogen phosphate $VOHPO_4 \cdot 0.5H_2O$, is the active component of these catalysts. Recently, the applicability of these samples to perform other reactions has been demonstrated, for example, the oxidation of *n*-pentane to maleic anhydride and phthalic anhydride [8–12], the partial oxidation of propane to acrylic acid [8, 13, 14], and the oxidative dehydrogenation of ethane and propane to ethylene and propylene, respectively [15–18]. The use of a fluidized catalyst bed is promising for the implementation of these processes, as demonstrated for the reaction of *n*-butane oxidation [8, 19–21]. This technological process is associated with the development of supported catalysts whose mechanical strength depends on the properties of the support. These catalysts are also promising for the use in fixed-bed reactors because they make it possible to decrease heating in the catalyst bed, to improve the temperature profile along the bed, and to decrease the consumption of active components for catalyst preparation. On the other hand, the use of a fluidized bed allows one to use the recycling of reaction mixtures enriched in a hydrocarbon and thus to improve the output of the target product [8]. Unfortunately, currently available data indicate that an increase in hydrocarbon concentration results in a decrease in the yield of the product and impairs the stability of catalyst operation. Thus, the development of VPO catalysts for operations in mixtures with an excess of paraffin is of considerable current interest.

Attempts to synthesize VPO catalysts with the use of various methods for supporting an active phase and chemically different supports, such as SiO_2, TiO_2, Al_2O_3, and metal phosphates, have been made repeatedly [22–28]. However, it was found that α-, β-, and ω-$VOPO_4$ phases or amorphous VPO compound phases resulted from the supporting an active VPO component [24–26], and these phases are ineffective in the oxidation of paraffin hydrocarbons [1, 3, 8]. The exception is a study by Li et al. [29], who synthesized VPO catalysts containing the vanadyl pyrophosphate phase based on pyrogenic silica.

Thus, with consideration for the possibility described by Li et al. [29], the preparation of active VPO phases supported on various carriers, including pyrogenic silicas, has not been sufficiently well substantiated experimentally. In this context, in this work, we studied the synthesis of supported catalysts with the use of both a traditional preparation procedure (in an excess of an organic solvent with varying the step of introducing the support, the natures of the support and the reducing agent, and the degree of reduction of

the initial vanadium oxide [29]) and nontraditional barothermal and mechanochemical techniques, which do not require the use of a large excess of a solvent or a reducing agent.

EXPERIMENTAL

The following starting reagents were used for the synthesis of VPO samples: V_2O_5 (analytical grade), 85% H_3PO_4 (analytical grade), and citric acid (analytical grade) or oxalic acid (analytical grade) as a reducing agent. The synthesis was performed in an *n*-butanol (analytical grade) solution in accordance with a procedure analogous to that published elsewhere [30]. In the synthesis of some samples, V_2O_5 mechanochemically pretreated in a Fritsch Pulverisette-6 ball planetary mill (balls 10 mm in diameter and a vessel of tungsten carbide; the ratio between the weight of balls and the weight of the oxide was 10 : 1; water was a treatment medium; rate, 600 rpm; treatment times, 30 and 60 min) was used. It is well known [31] that this treatment leads to the partial reduction of vanadium oxide; therefore, a reducing agent was not used in the course of synthesis with the pretreated V_2O_5 as the reagent.

For comparison, bulk VPO samples were synthesized (atomic ratio P/V = 1.15; weight ratio *n*-butanol/V_2O_5 = 9). After the separation of the solvent, these samples were subjected to thermal vacuum treatment at a residual pressure of 0.010–0.012 MPa with a gradual increase in the temperature to 270 and 300°C.

Pyrogenic aerosils A-300 (S_{sp} = 300 m^2/g) and A-50 (S_{sp} = 50 m^2/g) and TiO_2 with S_{sp} = 62 m^2/g, which was a mixture of anatase and rutile crystal modifications, were used as supports.

The following three methods were used for the synthesis of VPO samples:

(A) In the preparation of samples VPO-A1–VPO-A9, the synthesis was performed using a traditional procedure analogously to preparation conditions of bulk samples. In this procedure, a support was introduced into the reaction mixture either at the beginning of the synthesis (together with the starting reagents) or at the end of the synthesis analogously to a published procedure [29] (after the preparation of a VPO phase). In the latter case, the synthesis was continued for another 1 h. Simultaneously, the nature of the reducing agent and the degree of reduction of the initial vanadium oxide were varied in the course of synthesis using the mechanically preactivated sample (see above).

(B) The barothermal synthesis of supported samples (VPO-B1–VPO-B5) was performed in 45-ml laboratory autoclaves with Teflon inserts. The following starting reagents were thoroughly mixed in a glass beaker: V_2O_5, 85% H_3PO_4 (atomic ratio P/V = 1.15), a reducing agent, a support, and *n*-butanol (weight ratio support/*n*-butanol = 0.2). The resulting mixture was placed in a Teflon insert. To produce pressure in the autoclave, *n*-butanol was placed at the bottom. The synthesis was performed at 170°C and 0.5 MPa for 7 h. The pressure in the system was calculated using the Antoine equation [32].

After completion of the synthesis, all of the supported VPO systems were subjected to thermal vacuum treatment at a residual pressure of 0.010–0.012 MPa and a gradual increase in the temperature to 270 or 300°C.

(C) The mechanochemical synthesis of supported samples (VPO-MC) was performed by treating a mixture of vanadyl hydrogen phosphate prepared in accordance with a standard procedure with pyrogenic aerosil A-300 or TiO_2 for 60 min in air in a Fritsch Pulverisette-6 ball planetary mill (balls 10 mm in diameter and a 250-ml vessel of Si_3N_4; the ratio between the weight of balls and the weight of oxides was 13 : 1; rate, 600 rpm).

Table 1 summarizes the conditions of catalyst preparation. In all cases, the amount of a supported VPO phase was 30 wt %.

The synthesized samples were studied by XRD analysis on a DRON-4.0 diffractometer with the use of CuK_α radiation. The specific surface areas (S_{sp}) of the samples were measured by chromatography (Gazokhrom-1) based on the thermal desorption of argon. The total pore volume (V_Σ) was determined from the adsorption of water by the samples, which were dried in air at 100°C (sample weights of 0.5–1.0 g). The isotherms of nitrogen adsorption were measured at liquid nitrogen temperature on a Quantachrome NovaWin2 instrument. The electronic spectra were obtained on a Specord M 40 UV–vis spectrophotometer. The EPR spectra were measured on an X-band (wavelength of 3 cm) SEPR-03 instrument (PO Svetlana, Russia) at room temperature.

The catalytic experiments were performed in a flow-type system with a steel microreactor (6 mm in diameter and 10 cm in length). The loaded catalyst amount was 0.5 cm^3 (fraction of 0.25–0.50 mm). The initial components and reaction products were analyzed in the on-line mode using Chrom-5 and Selmi chromatographs analogously to a published procedure [33].

The selective oxidation of *n*-butane was studied using an enriched mixture (3.4 vol % in air) over the temperature range of 200–400°C at contact times of 0.5–2.4 s. The catalyst was activated in the working mixture for 8 h at 440°C.

The oxidative dehydrogenation of ethane was performed with the use of a mixture of $C_2H_6 : O_2 : He$ = 7 : 3 : 90 vol % over the temperature range of 370–500°C at contact times of 0.6–1.5 s. The catalyst was activated in the working mixture for 8 h at 550°C.

Table 1. Conditions of the synthesis of supported VPO catalysts*

Catalyst	Support	Support introduction time	Reducing agent	Sample reduction temperature, °C	Sample color
VPO-M1	–	–	CA	270	Green
VPO-M2	–	–	CA	300	Green
VPO-A1	A_{300}	SE	CA	270	Grayish blue
VPO-A2	A_{300}	SE	CA	300	Grayish blue
VPO-A3	A_{300}	SB	OA	270	Light green
VPO-A4	A_{300}	SB	OA	300	Gray
VPO-A5	A_{300}	SE	OA	270	Brown
VPO-A6	A_{300}	SE	OA	300	Black
VPO-A7***	A_{300}	SB	OA	270	Gray
VPO-A8***	A_{300}	SB	–	270	Gray
VPO-A9	A_{50}	SB	OA	270	Grayish blue
VPO-A10	TiO_2	SB	OA	270	Grayish blue
VPO-B1	A_{50}	SB	OA	270	Gray
VPO-B2**	A_{50}	SB	–	270	Gray
VPO-B3**	TiO_2	SB	–	270	Gray
VPO-B4***	A_{50}	SB	–	270	Light gray
VPO-B5***	TiO_2	SB	–	270	Grayish blue
VPO-MC1	A_{300}	SB	–	270	Light gray
VPO-MC2	TiO_2	SB	–	270	Light gray

* Support introduction time: (SE) at the end of the synthesis or (SB) at the beginning of the synthesis. Reducing agent: (CA) citric acid or (OA) oxalic acid.

**V_2O_5 after mechanochemical treatment for 30 min was used.

***V_2O_5 after mechanochemical treatment for 60 min was used.

RESULTS AND DISCUSSION

Table 2 summarizes the results of the study of the phase composition of the synthesized supported samples, and Fig. 1 shows characteristic examples of XRD patterns. It can be seen that, in the majority of cases, a supported phase of vanadyl hydrogen phosphate $VOPO_4 \cdot 0.5H_2O$ was formed as a result of the synthesis. The exception is represented by the following samples: VPO-A5, in which the phase of vanadyl pyrophosphate $(VO)_2P_2O_7$ was present; VPO-A6; VPO-B5; and VPO-MC2, a constituent of which was an X-ray amorphous VPO compound. With the use of TiO_2 as a support, the presence of reflections due to titanium dioxide (rutile + anatase) was also found in all of the samples. A halo characteristic of aerosil was observed in all of the XRD patterns of the samples synthesized with the use of aerosil as a support (e.g., see Figs. 1b–1d).

The experimental results indicate that the nature of the support had no effect on the phase composition of the sample when preparation method A was used. Citric acid is a weaker reducing agent than oxalic acid, as evidenced by the presence of V/P micas (compounds containing V^{5+} and V^{4+} ions) in sample VPO-A1. An increase in the vacuum treatment temperature resulted in their conversion into vanadyl hydrogen phosphate. It was found that the introduction of a support at the end of the synthesis made it possible to obtain a supported phase of vanadyl pyroposphate (VPO-A5 and A6 samples; Table 2 and Fig. 1c), which has not been described previously in the literature. This is likely due to the fact that aerosil, which was introduced into the system after the completion of VPO phase formation, exhibited dehydrating properties in the subsequent thermal treatment. As we assumed, the use of mechanochemically pretreated V_2O_5 in the synthesis (samples VPO-A7 and VPO-A8; Table 2 and Fig. 1d) allowed us to synthesize supported vanadyl hydrogen phosphate without the use of a reducing agent. As can been in Table 2, sample VPO-A8 was identical to the sample synthesized with the addition of oxalic acid (VPO-A7) in its characteristics.

With the use of synthesis method B (Table 2), a supported vanadyl hydrogen phosphate was obtained in all cases (with the exception of sample VPO-B5). As in the previous case, the use of V_2O_5 subjected to mechanical pretreatment allowed us to exclude a reducing agent from the synthesis of catalysts. At the same time, note that the reduction of vanadium oxide in the preliminary mechanical treatment led to the formation of an amorphous VPO phase on a TiO_2 sup-

Table 2. Structure and catalytic properties of supported VPO samples*

Sample	S_{sp}, m^2/g	V_Σ, cm^3/g	d, nm	VPO phase	I_{001}/I_{220}	D, nm	Number of VPO-phase monolayers	$w_{C_4H_{10}} \times 10^3$, mol h^{-1} g^{-1}	$w_{C_2H_6} \times 10^3$, mol h^{-1} g^{-1}
VPO-M1	25	–	–	$VOHPO_4$	0.47	23	–	1.4	4.9
VPO-M2	21	–	–	$VOHPO_4$	0.68	24	–	2.1	4.4
VPO-A1	214	0.91	17.0	$VOHPO_4$ + V/P micas	0.56	20	3	7.8	–
VPO-A2	151	0.99	26.5	$VOHPO_4$	0.81	23	4	15.2	35.7
VPO-A3	226	1.51	26.7	$VOHPO_4$	0.40	23	3	9.8	44.1
VPO-A4	182	1.45	32.0	$VOHPO_4$	0.74	24	4	13.0	36.7
VPO-A5	198	1.04	21.0	$(VO)_2P_2O_7$	–	16	–	17.6	41.6
VPO-A6	161	0.91	22.5	$(VO)_2P_2O_7$	–	18	–	30.7	40.8
VPO-A7***	69	0.64	37.0	$VOHPO_4$	0.58	39	9	10.3	37.7
VPO-A8***	89	0.65	29.0	$VOHPO_4$	0.75	30	7	11.5	33.6
VPO-A9	46	0.93	81.0	$VOHPO_4$	0.70	28	14	12.2	35.8
VPO-A10	28	0.46	65.7	$VOHPO_4 + TiO_2$	0.95	23	24	4.2	29.6
VPO-B1	50	1.05	84.0	$VOHPO_4$	0.93	32	13	11.4	28.5
VPO-B2**	44	0.72	65.5	$VOHPO_4$	0.76	30	15	13.4	42.2
VPO-B3**	28	0.71	101	$VOHPO_4 + TiO_2$	1.43	23	24	10.4	42.5
VPO-B4***	43	0.71	66.0	$VOHPO_4$	0.77	35	15	13.2	–
VPO-B5***	30	0.62	82.5	$A+TiO_2$	–	–	–	4.0	24.8
VPO-MC1	130	–	–	$VOHPO_4$	0.75	23	5	13.6	41.3
VPO-MC2	23	–	–	$A + TiO_2$	–	–	–	3.7	18.2

* S_{sp} is the specific surface area; V_Σ is the total pore volume; d is the average pore size; D is the crystallite size; $VOHPO_4 = VOHPO_4 \cdot 0.5H_2O$; A is an amorphous phase; and $w_{C_4H_{10}}$ and $w_{C_2H_6}$ are the rates of oxidation of *n*-butane and ethane at 350 and 500°C, respectively, per gram of the active component.

port (cf. samples VPO-B3 and VPO-B5). An analogous behavior was also observed in the mechanochemical synthesis with the use of TiO_2: the XRD pattern exhibited only reflections from the support (Fig. 1e), whereas a vanadyl hydrogen phosphate phase was formed after mechanochemical treatment in the case of aerosil (sample VPO-MV1, Fig. 1d).

The XRD data (Table 2) indicate that, in all of the samples containing a supported phase of vanadyl hydrogen phosphate, the main reflections belonged to the planes (001) and (220); in this case, a reflection from the side plane (220) exhibited a maximum intensity (sample VPO-B3 was the exception). An increase in the vacuum treatment temperature resulted in an increase in the I_{001}/I_{220} ratio. On the other hand, note that, in supported catalysts, the reflection intensity from the basal plane (001) was higher than that of a bulk analog. The crystallite sizes of the VPO phase calculated from the Scherer equation [34] were 20–30 nm, and they are not very different from those in the samples prepared under various conditions (Table 2).

As follows from the data given in Table 2, the supporting of a VPO phase resulted in a decrease in the S_{sp} of the support in all cases. As the vacuum treatment temperature was increased, this decrease became more significant. The addition of a support at the end of the catalyst synthesis resulted in a greater decrease in S_{sp} than upon the introduction of the support into the system at the beginning of the synthesis (see samples VPO-A1 and VPO-A2 or VPO-A3 and VPO-A5, respectively). Note that the S_{sp} of all of the supported VPO samples was higher than that of the bulk samples. With the use of the values of S_{sp} and published data [35] on the structural parameters of the $VOHPO_4 \cdot 0.5H_2O$ phase ($a = 0.741$ nm, $b = 0.56$ nm, and $c = 0.959$ nm) and taking into account the intensity ratio between basal and side planes (Table 2), we calculated the surface coverage of the support with the VPO phase (the value of S_{sp} for a supported sample was used in the calculation). As can be seen in Fig. 2, a linear correlation between the amount of supported phase monolayers (m) and the reciprocal of S_{sp} was observed regardless of the synthesis method and the support

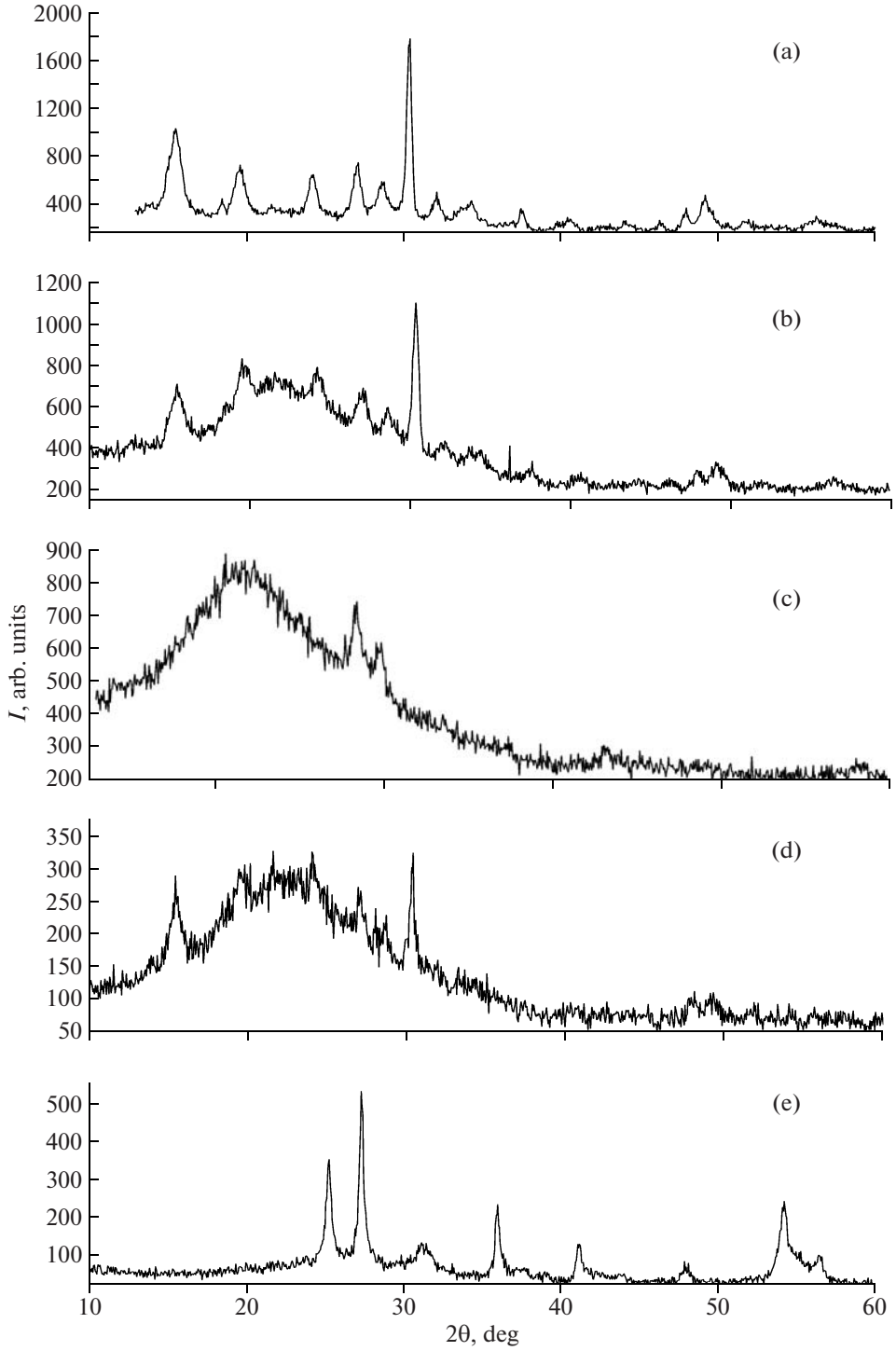

Fig. 1. X-ray diffraction patterns of the synthesized VPO samples: (a) bulk VPO-M1 and supported (b) VPO-A1, (c) VPO-A5, (d) VPO-MC1, and (e) VPO-MC2.

surface coverage with an active phase was the same at similar specific surface areas (Fig. 2 and Table 2).

The measurements of the pore volumes of the samples showed that initially nonporous pyrogenic supports became porous systems upon supporting a VPO phase. We found that individual support A-300 treated under conditions analogous to those for the synthesis of samples VPO-A1 or VPO-A3 exhibited S_{sp} of 260 m^2/g at a pore volume of 1.78 cm^3/g and an average pore diameter of 27.0 nm. The pore size (d_{av}) was calculated from the equation $d_{av} = 4V_{\Sigma}/S_{sp}$, where V_{Σ} is the total pore volume [36]. Table 2 summarizes

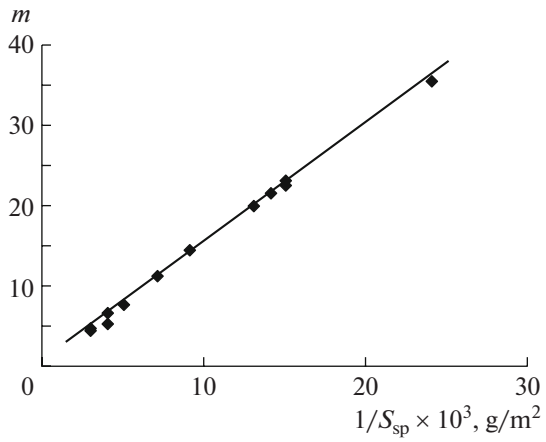

Fig. 2. Dependence of the number of monolayers of a supported active phase (m) on the reciprocal of the specific surface area of the support.

the results. A comparison between these data indicates that, upon the introduction of the support at the end of the synthesis, the pore structure of the support was filled with the resulting VPO phase. As a result, both the pore volume and the pore diameter decreased (cf. samples VPO-A3 and VPO-A5 or VPO-A4 and VPO-A6). An increase in the vacuum treatment temperature resulted in an increase in the pore size; this allowed us to hypothesize the filling of micropores with the VPO phase or the "closure" of pores.

Form the isotherms of N_2 adsorption, it follows that micropores with radii smaller than 1 nm were absent from the catalysts. In addition, it was found that the total pore volume was much smaller than V_Σ determined by gravimetry. Thus, for example, it was 0.2 cm^3/g for VPO-A2, whereas gravimetry afforded a value of 0.9 cm^3/g (Table 2). This fact allowed us to assume that the main pore volume belongs to macropores. Consequently, if these samples will be used in catalytic processes, internal diffusion limitations will be absent.

Although the synthesized catalysts were differently colored, their UV–VIS spectra were similar and exhibited an absorption band at 650 nm, which suggested the presence of V^{4+} ions in the samples [37].

The presence of a considerable number of V^{4+} ions in the samples was also supported by EPR spectra (Fig. 3) as a broad singlet, which characterizes the occurrence of exchange and dipole–dipole interactions between ions. The spectrum of a bulk sample of vanadyl hydrogen phosphate (Fig. 3a) exhibited a characteristic asymmetrical signal [4, 24, 26, 38] with the width $\Delta H = 125$ G and the g factor of 1.955. The signal asymmetry was explained by a considerable distortion in the octahedral coordination of vanadium ions because of the presence of coordinated water molecules in the interlayer spacing. In this sample, the signal intensity was 2.1×10^{21} spin/g, which is close to

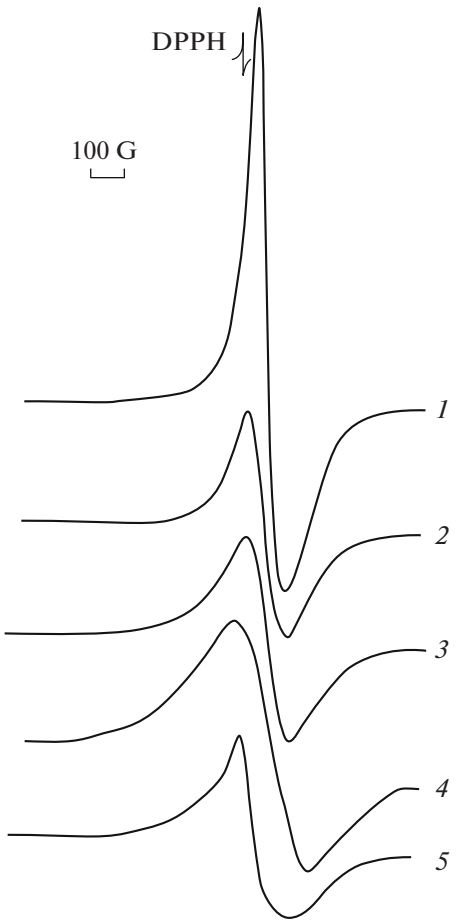

Fig. 3. EPR spectra of the synthesized samples: (*1*) bulk VPO-M2 and supported (*2*) VPO-A3, (*3*) VPO-A5, (*4*) VPO-A9, and (*5*) VPO-B3.

the theoretical concentration of vanadium ions of 2.5×10^{21} spin/g. The supporting of the vanadyl hydrogen phosphate phase as a thin layer onto a support (sample VPO-A3, Table 2) resulted in the removal of asymmetry (Fig. 3b), a signal broadening ($\Delta H = 145$ G), and an insignificant change in the g factor to 1.960. The signal intensity was about 25% of the signal intensity of the bulk analog. As the amount of the supported VPO phase was increased (VPO-A10 sample), the signal width increased (Fig. 2d) to $\Delta H = 195$ G with no changes in the g factor and intensity. The spectrum of a sample containing an amorphous VPO phase on the support surface (VPO-B5) exhibited a symmetrical signal with the same intensity and g factor but with the width $\Delta H = 160$ G. The EPR spectrum of supported vanadyl pyrophosphate (VPO-A5) contained a symmetrical singlet with $g = 1.960$, $\Delta H = 150$ G, and an intensity of 0.6×10^{21} spin/g.

The study of n-butane oxidation demonstrated that maleic anhydride and carbon oxides (CO and CO_2) were reaction products on both the supported and bulk catalysts. It was found that vanadyl hydrogen phosphate was converted into vanadyl pyrophosphate in

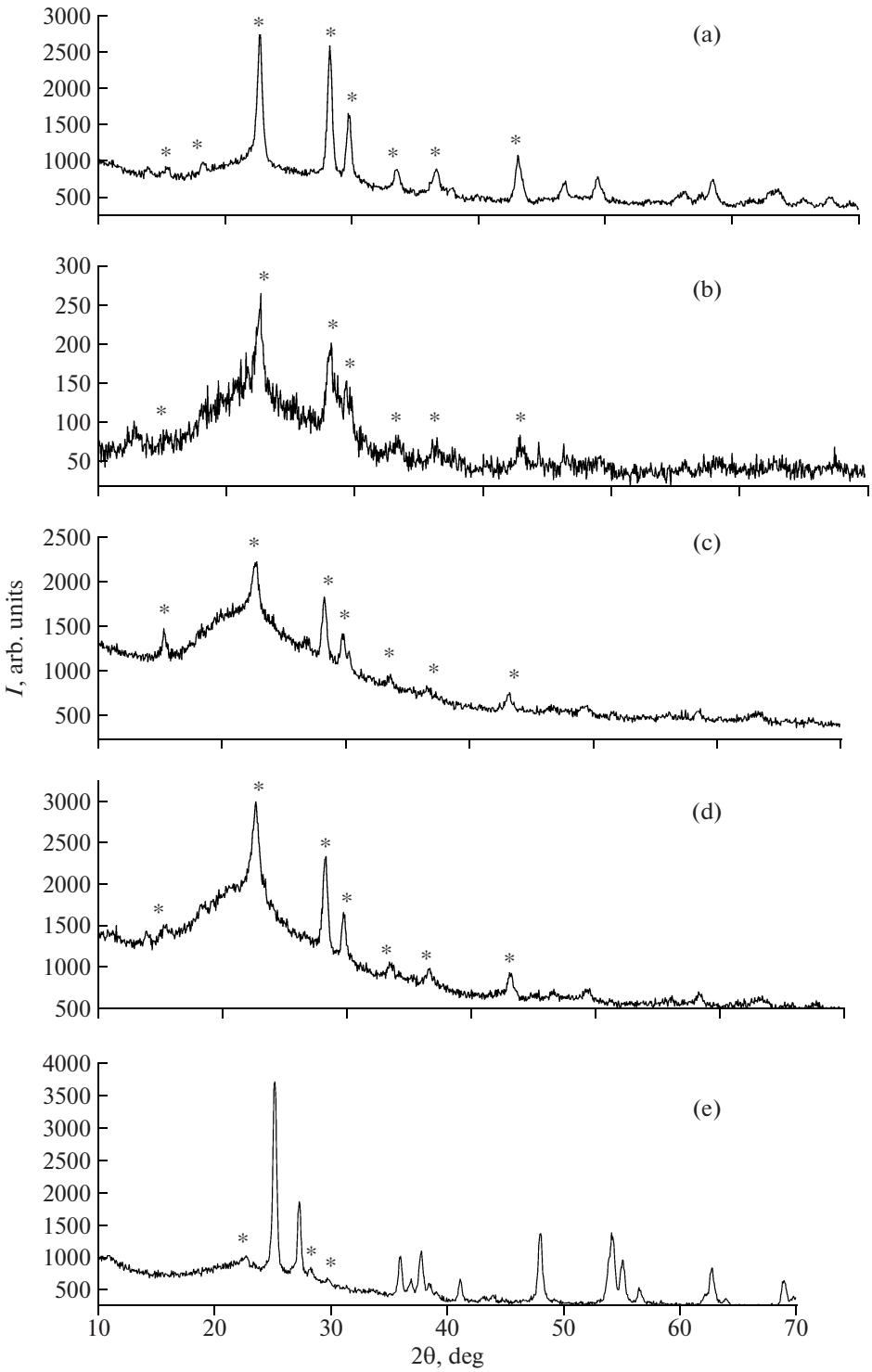

Fig. 4. X-ray diffraction patterns of the VPO samples after *n*-butane oxidation ((a) bulk VPO-M1 and (b) VPO-A6) and ethane oxidative dehydrogenation ((c) VPO-A9, (d) VPO-B2, and (e) VPO-B3); (*) reflections from the vanadyl pyrophosphate phase.

the course of catalysis (Fig. 4). Table 2 summarizes the rates of *n*-butane oxidation per unit active weight; these data indicate that the activity of a bulk catalyst in a reaction mixture with a high hydrocarbon concentration was much lower than the activity of supported samples. In this case, we can note that the reaction rate of oxidation on supported catalysts generally increased with increasing basal plane content (Fig. 5). The samples in the synthesis of which a vanadyl pyrophosphate phase was initially obtained (VPO-A5 and

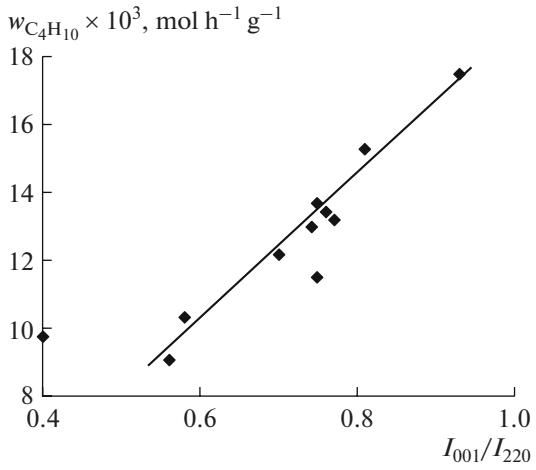

Fig. 5. Dependence of the rate of *n*-butane oxidation (350°C) on the reflection intensity ratio I_{001}/I_{220} of the $VOHPO_4 \cdot 0.5H_2O$ phase in supported catalysts.

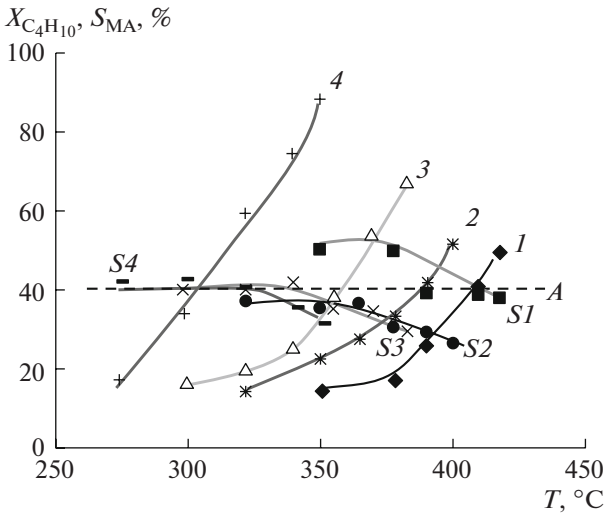

Fig. 6. Dependence of *n*-butane conversion ($X_{C_4H_{10}}$) and selectivity for maleic anhydride formation (S_{MA}) on the reaction temperature: (*1, S1*) VPO-M1, (*2*, *S2*) VPO-A3, (*3*, *S3*) VPO-A2, and (*4*, *S4*) VPO-A6. Contact time: 1.2 s.

VPO-A6) exhibited a maximum activity in *n*-butane oxidation. Figures 6 and 7 show data on the conversion of the hydrocarbon and the selectivity of maleic anhydride formation on test samples. The conversion of *n*-butane on a bulk sample in a reaction mixture with a high hydrocarbon concentration was much lower than that on the supported samples synthesized using method A (Fig. 6). At the same time, the selectivity of maleic anhydride formation on the bulk catalyst was higher than that on the supported samples. Note that the selectivity values were similar at the same conversion of *n*-butane (~40%, line *A* in Fig. 6) on both the bulk and supported catalysts; however, they were reached at much lower temperatures in the latter case. The decrease in the reaction characteristics of *n*-butane oxidation with the use of mixtures enriched in the hydrocarbon is well known from published data [39–42]. Thus, Kamiya et al. [41] found that the yield of maleic anhydride on the bulk VPO catalyst at 390°C and an *n*-butane concentration of 3–5 vol % was 11%. Somewhat better characteristics were obtained by Mallada and coauthors [40, 42]: 17.7% at 400°C. In our case, the product yield on the bulk VPO catalyst at 420°C was as high as 18%, whereas higher yields of maleic anhydride were obtained on the supported catalysts synthesized using method A (21 and 24% on samples VPO-A2 and VPO-A6, respectively) at lower temperatures of 380 and 330°C, respectively.

Data shown in Fig. 7 indicate that the conversion of *n*-butane on supported VPO samples synthesized using methods B and C was much higher than that on the bulk analog. At the same degrees of *n*-butane conversion (line *A* in Fig. 7), the selectivity of maleic anhydride formation on these samples was higher than that on the bulk VPO catalyst. In this case, the above dependence (Fig. 5) of the activity on the basal plane content of the catalyst was also observed. The supported catalysts synthesized with the use of TiO_2 were worse than the samples on aerosil in performance characteristics. Note that supported catalyst VPO-MC1, which was prepared by the mechanochemical treatment of vanadyl hydrogen phosphate and aerosil, exhibited a high efficiency. The yields of maleic anhydride on samples VPO-B1 and VPO-MC1 were 24 and 26%, respectively.

In the oxidation of ethane, the conversion of vanadyl hydrogen phosphate into an active phase of vanadyl pyrophosphate occurred analogously to the above process (Fig. 3). Ethylene was the main product of this reaction; consequently, the oxidative dehydro-

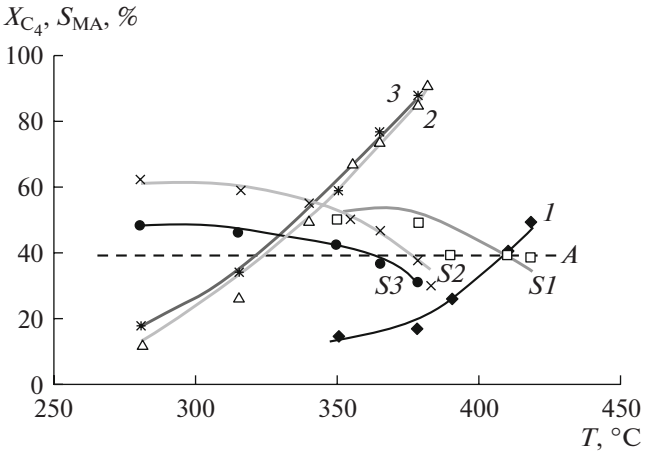

Fig. 7. Dependence of *n*-butane conversion (X_{C_4}) and selectivity for maleic anhydride formation (S_{MA}) on the reaction temperature: (*1*, *S1*) VPO-M1, (*2*, *S2*) VPO-MC1, and (*3*, *S3*) VPO-B2. Contact time: 1.2 s.

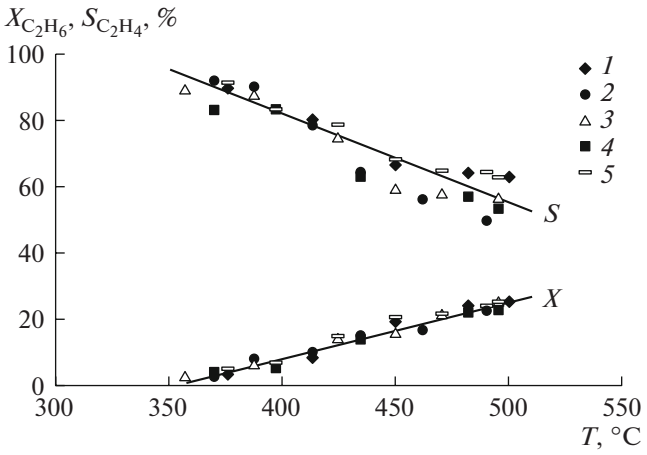

Fig. 8. Dependence of ethane conversion ($X_{C_2H_6}$) and selectivity for ethylene formation ($S_{C_2H_6}$) on the reaction temperature: (*1*) VPO-M1, (*2*) VPO-A9, (*3*) VPO-B2, (*4*) VPO-B3, and (*5*) VPO-MC1. Contact time: 0.6 s.

genation of ethane occurred. According to the results summarized in Table 2, the rate of ethane oxidation per unit active weight on supported catalysts was higher than the values reached on bulk samples. At the same time, data on the dependence of ethane conversion and selectivity for ethylene formation on the reaction temperature (Fig. 8) indicate that, regardless of the nature of the support and the method used for sample preparation, the supported catalysts afforded performance characteristics analogous to those obtained on the bulk VPO catalyst. The yield of ethylene at 500°C was close to 12% on both bulk and supported catalysts. Consequently, the use of supported VPO catalysts in this reaction makes it possible not only to decrease the consumption of active components for catalyst preparation but also to increase their mechanical strength and, probably, to improve temperature profiles in large-diameter reactors with no increase in reaction characteristics.

Thus, in this work, we found that traditional synthesis in organic solvents with the addition of a support allowed us to obtain supported VPO phases; this is consistent with published data [29]. In this case, we found that the composition of this phase depends on the time taken to introduce the support into the reaction mixture and on the temperature of the thermal treatment of the resulting sample. The use of mechanochemically pretreated V_2O_5 in traditional synthesis allowed us to exclude the use of a reducing agent. We found that the replacement of the traditional method for the preparation of supported catalysts with a barothermal synthesis allowed us to obtain active supported VPO phases and to decrease the used amount of an organic solvent by a factor of more than 10 on the removal of a reducing agent from the synthesis. Direct mechanochemical synthesis is promising for the preparation of supported VPO catalysts; it provides an opportunity to improve the reaction characteristics of *n*-butane oxidation at elevated hydrocarbon concentrations with no changes in the catalytic properties of these samples in the oxidative dehydrogenation reaction of ethane, as compared with bulk VPO catalysts. Simultaneously, note that the supported catalysts prepared in this work were better than the well-known VPO catalysts supported on SiO_2 in terms of performance characteristics in both the oxidation of *n*-butane [43, 44] and the oxidative dehydrogenation of ethane [45].

REFERENCES

1. Hodnett, B.K., *Catal. Rev. Sci. Eng.*, 1985, vol. 27, no. 3, p. 373.
2. Shimoda, T., Okuhara, T., and Misono, M., *Bull. Chem. Soc. Jpn.*, 1985, vol. 58, no. 8, p. 2163.
3. Zazhigalov, V.A., *Katal. Katalizatory*, 1985, no. 23, p. 17.
4. Centi, G., Trifiro, F., Ebner, J.R., and Franchetti, V.M., *Chem. Rev.*, 1988, vol. 88, no. 1, p. 55.
5. Bordes, E., *Catal. Today*, 1993, vol. 16, no. 1, p. 27.
6. Albonetti, S., Cavani, F., and Trifiro, F., *Catal. Rev. Sci. Eng.*, 1996, vol. 38, no. 4, p. 413.
7. Volta, J.C., *Surf. Chem. Catal.,* 2000, no. 3, p. 717.
8. Centi, G., Cavani, F., and Trifiro, F., *Selective Oxidation by Heterogeneous Catalysis*, New York: Plenum, 2001.
9. Krylov, O.V., *Geterogennyi kataliz* (Heterogeneous Catalysis), Moscow: Akademkniga, 2004.
10. Sobalik, Z., Gonzalez, S., and Ruiz, P., *Stud. Surf. Sci. Catal.,* 1995, vol. 91, p. 727.
11. Zazhigalov, V.A., Haber, J., Stoch, J., Mikhajluk, B.D., Pyatnitskaya, A.I., Komashko, G.A., and Bacherikova, I.V., *Catal. Lett.*, 1996, vol. 37, no. 1, p. 95.
12. Zazhigalov, V.A., Cheburakova, E.V., Genser, M., and Stokh, E., *Kinet. Katal.*, 2006, vol. 47, no. 6, p. 827 [*Kinet. Catal.* (Engl. Transl.), vol. 47, no. 6, p. 803].
13. Ai, M., *J. Catal.*, 1986, vol. 101, no. 2, p. 389.
14. Gribot-Perrin, N., Volta, J.-C., Burrows, A., Kiely, C., and Gubelmann-Bonneau, M., *Stud. Surf. Sci. Catal.*, 1996, vol. 101, p. 1205.
15. Takita, Y., Yamashita, H., and Moritaka, K., *Chem. Lett.,* 1989, no. 10, p. 1733.
16. Michalakos, P.M., Kung, M.C., Jahan, I., and Kung, H.H., *J. Catal.,* 1993, vol. 140, no. 2, p. 226.
17. Gasior, M., Gressel, I., Zazhigalov, V.A., and Grybowska, B., *Pol. J. Chem.*, 2003, vol. 77, no. 7, p. 909.
18. Solsona, B., Zazhigalov, V.A., Lopez-Nieto, J.M., Bacherikova, I.V., and Diyuk, E.A., *Appl. Catal., A*, 2003, vol. 246, no. 1, p. 81.
19. Contractor, R.M. and Sleight, A.W., *Catal. Today*, 1987, vol. 1, no. 4, p. 587.
20. Haggin, J., *Chem. Eng. News,* 1995, no. 3, p. 20.
21. Cavani, F., Bacchini, M., Cortesi, S., Ligi, S., Pierelli, F., Trifiro, F., and Mazzoni, G., *4th World Congr. on Catalysis*, 2001, vol. 1, p. 83.

22. Roy, M., Gubelmann-Bonneau, M., Ponceblanc, H., and Volta, J.C., *Catal. Lett.*, 1996, vol. 42, no. 1, p. 93.
23. Bethke, G.K., Wang, D., Bueno, J.M.C., Kung, M.C., and Kung, H.H., *Stud. Surf. Sci. Catal.*, 1997, vol. 110, p. 453.
24. Zazhigalov, V.A., Bogutskaya, L.V., Lyashenko, L.V., and Bacherikova, I.V., *Stud. Surfr. Sci. Catal.*, 1997, vol. 110, p. 787.
25. Santamaria-Gonzalez, J., Martinez-Lara, M., Banares, M.A., Martinez-Huerta, M.V., Rodriguez-Castellon, E., Fierro, J.L.G., and Jeminez-Lopez, A., *J. Catal.,* 1999, vol. 181, no. 2, p. 280.
26. Ruitenbeek, M., *Characterisation of Vanadium-Based Oxidation Catalysts: Thesis*, Utrecht: Univ. of Utrecht, 1999.
27. Guliants, V.V., Benziger, J.B., Sundaresan, S., and Wachs, I.E., *Stud. Surf. Sci. Catal.*, 2000, vol. 130, p. 1721.
28. Ciambelli, P., Galli, P., Lisi, L., Massucci, M.A., Patrono, P., Pirone, R., Ruoppolo, G., and Russo, G., *Appl. Catal., A*, 2000, vol. 203, no. 1, p. 133.
29. Li, X.K., Ji, W.J., Zhao, J., Zhang, Z., and Au, C.T., *Appl. Catal., A*, 2006, vol. 306, no. 1, p. 8.
30. Zazhigalov, V.A., Haber, J., Stoch, J., Pyatnitskaya, A.I., Komashko, G.A., and Belousov, V.M., *Appl. Catal., A*, 1993, vol. 96, no. 1, p. 135.
31. Zazhigalov, V.A., Haber, J., Stoch, J., Kharlamov, A.I., Bogutskaya, L.V., Bacherikova, I.V., and Kowal, A., *Solid State Ionics*, 1997, vols. 101–103, p. 1257.
32. Reid, R., Prausnitz, J., and Sherwood, T., *The Properties of Gases and Liquids*, New York: McGraw-Hill, 1977.
33. Zazhigalov, V.A., Pyatnitskaya, A.I., Komashko, G.A., and Belousov, V.M., *Neftekhimiya,* 1980, vol. 20, no. 1, p. 94.
34. Kameron, G.Kh. and Patterson, A.L., *Usp. Fiz. Nauk*, 1939, vol. 22, no. 4, p. 442.
35. Gai, P.L., *Curr. Opin. Solid State Mater. Sci.*, 1999, vol. 4, no. 1, p. 63.
36. Gregg, S.J. and Sing, K.S.W., *Adsorption, Surface Area and Porosity*, London: Academic, 1967.
37. Villeneuve, G., Erragh, A., and Beltran, D., *Mater. Res. Bull.*, 1986, vol. 21, no. 4, p. 621.
38. Zazhigalov, V.A., Belousov, V.M., Ladvig, G., Komashko, G.A., and Pyatnitskaya, A.I., *Ukr. Khim. Zh.*, 1988, vol. 54, no. 1, p. 35.
39. Ballarini, N., Cavani, F., Cortelli, C., Ligi, S., Pierelli, F., Trifiro, F., and Fumagalli, C., *Top. Catal.*, 2006, vol. 38, no. 2, p. 147.
40. Mallada, R., Sajip, S., Kiely, C.J., Menendez, M., and Santamaria, J., *J. Catal.,* 2000, vol. 196, no. 1, p. 1.
41. Kamiya, Y., Nishikawa, E., Okuhara, T., and Hattori, T., *Appl. Catal., A,* 2001, vol. 206, no. 1, p. 103.
42. Mallada, R., Menendez, M., and Santamaria, J., *Catal. Today*, 2000, vol. 56, no. 2, p. 191.
43. US Patent 5932746, 1999.
44. US Patent 6362128, 2002.
45. US Patent 6914029, 2005.